The formal publication is available online via https://doi.org/10.1016/j.ijnonlinmec.2019.103308.

Multimodal vibration damping of nonlinear structures using multiple nonlinear absorbers

G. Raze[a,*], G. Kerschen[a]

[a]*Space Structures and Systems Laboratory, Aerospace and Mechanical Engineering Department, University of Liège Quartier Polytech 1 (B52/3), Allée de la Découverte 9, B-4000 Liège, Belgium*

Abstract

This paper presents a tuning methodology for multiple nonlinear vibration absorbers that mitigate several nonlinear resonances simultaneously. Specifically, the objective is to maintain equal peaks in the frequency response for all controlled resonances in an as large as possible range of forcing amplitudes. Relying on an all-equal-peak design for linear regimes of motion and adopting a principle of similarity for nonlinear regimes, a semi-analytical expression of the absorber coefficients is derived using first-order harmonic balance and a series expansion of the harmonic coefficients. The proposed methodology is demonstrated numerically using two spring-mass systems.

Keywords: tuned vibration absorber, multimodal vibration absorber, equal-peak method, principle of similarity, nonlinear vibrations

1. Introduction

More than a century ago, Frahm [1] invented the linear tuned vibration absorber (LTVA). This device is able to suppress a structural resonance by destructive interference at the corresponding frequency. Unfortunately, the frequency response of the controlled structure exhibits two high-amplitude resonance peaks around that suppression frequency. In order to reduce peak amplitudes, Ormondroyd and Den Hartog [2] added viscous damping to the absorber. Then, Brock [3] derived a closed-form expression for the damping coefficient. Their approach minimized (approximately) the maximum amplitude of the frequency response function, giving rise to the so-called *equal-peak method*. The exact solution to this problem was found by Nishihara and Asami [4].

Because the LTVA is tuned to a specific frequency, any variation in the host structure may detune the absorber, which, in turn, affects its performance. The nonlinear energy sink (NES), comprising a mass, a dissipative element and an essentially nonlinear stiffness, was proposed in [5, 6]

*Corresponding author
Email addresses: g.raze@uliege.be (G. Raze), g.kerschen@uliege.be (G. Kerschen)

as a remedy to this issue. Irreversible targeted energy transfer from the host structure to the absorber may take place regardless of the structural resonance frequency. The NES is, however, not efficient at low forcing amplitudes [7]. The tuned bistable nonlinear energy sink (TBNES) was proposed in [8] to address this limitation. Equipped with a negative linear stiffness, the TBNES reduces the energy threshold at which energy transfer occurs.

For nonlinear host structures, Agnes [9] found out that nonlinear absorbers have better performance than linear absorbers. Other studies discussed the merits and demerits of nonlinear absorbers on nonlinear systems, see, e.g., [10, 11, 12, 13, 14]. Viguie and Kerschen [15] derived a qualitative tuning rule for nonlinear tuned vibration absorbers (NLTVAs), i.e., the frequency-energy dependence of the absorber should be identical to that of the host structure. More recently, Habib et al [16] introduced a *nonlinear principle of similarity* to develop NLTVAs whose performance is much less sensitive to forcing amplitude. This principle states that the functional form of the NLTVA's nonlinearity should be identical to that of the host structure. If the nonlinear coefficient of the absorber is tuned adequately, the equal-peak method can be generalized to nonlinear regimes of motion, at least up to the merging of an isolated resonance [17]. Detroux et al. [18] studied the associated adverse dynamics and how the NLTVA parameters can be adapted to prevent such undesirable phenomena.

A more challenging scenario is when multiple resonances are to be mitigated. When several LTVAs are attached to a linear host structure, we proposed a so-called *all-equal-peak tuning rule* for which the controlled resonance peaks all feature the same amplitude [19]. A norm-homotopy optimization algorithm was thus proposed in this paper to compute the corresponding absorber parameters. Several studies addressed the case where an NES is used for mitigating sequentially several linear resonances, see, e.g., [20, 21]. However, there are very few studies dealing with multiple nonlinear absorbers attached to a nonlinear host.

In this context, the present paper introduces a tuning methodology for multiple NLTVAs that mitigate several nonlinear resonances simultaneously. Specifically, the objective is to maintain equal peaks in the frequency response for all controlled resonances in both linear and nonlinear regimes of motion. Section 2 briefly reviews the all-equal-peak design developed in [19], which is used herein for determining the linear parameters of the NLTVAs. In Section 3, the nonlinear principle of similarity is adopted, and an approximation of the nonlinear response of the controlled structure based on harmonic balance followed by a power series expansion yields a semi-analytical formula for the nonlinear coefficients of the absorbers. Section 4 demonstrates the resulting methodology using two numerical examples possessing two and five degrees of freedom, respectively. The conclusions of the present study are drawn in Section 5.

2. Tuning of Multiple Linear Tuned Vibration Absorbers

To ensure that the absorbers are efficient at low forcing amplitudes, their linear parameters are computed by removing all nonlinearities in the system. The governing equations of motion of a host structure possessing N degrees of freedom to which N_a LTVAs are attached are:

$$\begin{bmatrix} \mathbf{M}_0 & \mathbf{0} \\ \mathbf{0} & \mathbf{M}_a \end{bmatrix} \begin{bmatrix} \ddot{\mathbf{x}}_0 \\ \ddot{\mathbf{x}}_a \end{bmatrix} + \begin{bmatrix} \mathbf{C}_0 + \mathbf{B}\mathbf{C}_a\mathbf{B}^T & -\mathbf{B}\mathbf{C}_a \\ -\mathbf{C}_a\mathbf{B}^T & \mathbf{C}_a \end{bmatrix} \begin{bmatrix} \dot{\mathbf{x}}_0 \\ \dot{\mathbf{x}}_a \end{bmatrix} + \begin{bmatrix} \mathbf{K}_0 + \mathbf{B}\mathbf{K}_a\mathbf{B}^T & -\mathbf{B}\mathbf{K}_a \\ -\mathbf{K}_a\mathbf{B}^T & \mathbf{K}_a \end{bmatrix} \begin{bmatrix} \mathbf{x_0} \\ \mathbf{x}_a \end{bmatrix} = \begin{bmatrix} \mathbf{f} \\ \mathbf{0} \end{bmatrix}, \tag{1}$$

or, in short form,

$$\mathbf{M} \begin{bmatrix} \ddot{\mathbf{x}}_0 \\ \ddot{\mathbf{x}}_a \end{bmatrix} + \mathbf{C} \begin{bmatrix} \dot{\mathbf{x}}_0 \\ \dot{\mathbf{x}}_a \end{bmatrix} + \mathbf{K} \begin{bmatrix} \mathbf{x}_0 \\ \mathbf{x}_a \end{bmatrix} = \begin{bmatrix} \mathbf{f} \\ \mathbf{0} \end{bmatrix}, \tag{2}$$

where $\mathbf{M}$, $\mathbf{C}$ and $\mathbf{K}$ are the structural mass, damping and stiffness matrices, respectively. $\mathbf{x}$ is the vector of generalized coordinates. Subscripts 0 and a refer to the host structure and the absorbers, respectively. $\mathbf{f}$ is the vector of conjugated generalized forces. $\mathbf{B} = [\mathbf{b}_1 \ , \ \cdots \ , \ \mathbf{b}_{N_a}]$ collects the localization vectors $\mathbf{b}_n$ associated with the n^{th} absorber.

In the presence of harmonic forcing, the vibratory amplitude of the host structure is classically mitigated through the minimization of the H_∞ norm of a given transfer function, i.e., its maximum amplitude, resulting in the equal-peak design [2, 4]. The idea developed in [19] was to extend H_∞ minimization to multiple LTVAs by equating the amplitude of all controlled resonance peaks.

One inherent difficulty with the H_∞ norm is that it considers only the resonance peak exhibiting the largest amplitude, i.e., it disregards the other controlled peaks. Their amplitude is thus minimized later in the optimization process when they themselves feature the largest amplitude. This typically results in a nonsmooth cost function. The alternative strategy proposed in that paper relied on a norm-homotopy optimization during which problems of increasing complexity are solved sequentially using the previously-obtained parameters as an initial guess for the next problem. Specifically, the p-norm of the vector containing the controlled peak amplitudes, i.e., $\|x\|_p = \left(\sum_{i=1}^{n} |x_i|^p\right)^{1/p}$, is minimized, and p is sequentially increased so as to approach the H_∞ norm. A low value of p puts more weight on the resonance peaks with lower amplitudes, giving more chances to converge toward the all-equal-peak design. The subsequent increase in p ensures that resonances with large amplitudes are penalized enough. The flowchart of this approach, embedded in the tuning methodology proposed in this paper, is presented in Figure 3.

As an example, the outcome of the algorithm is illustrated with the two-degree-of-freedom example depicted in Figure 1. The system parameters are given in Section 4 (in this paper, every physical quantity has arbitrary units). Figure 2 shows the all-equal-peak design resulting from the norm-homotopy optimization algorithm, in which the peaks associated to the controlled structure are all equal in amplitude. Existing algorithms in the literature, see, e.g., [22], also enforce equal peaks for each resonance, but the amplitudes associated with each pair of peaks are not equal.

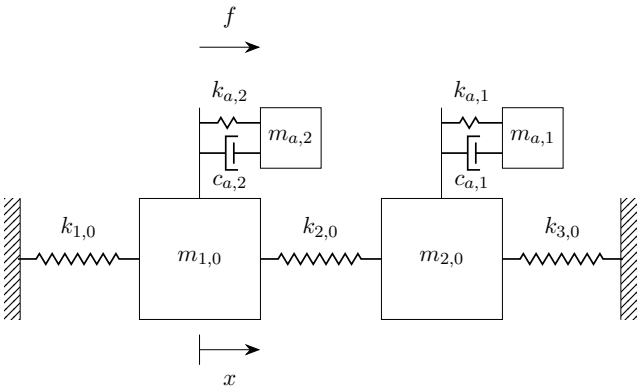

Figure 1: Two-degree-of-freedom system with two LTVAs.

3. Tuning of Multiple Nonlinear Tuned Vibration Absorbers

This section computes the nonlinearities of the NLTVAs so as to maintain equal peaks for all controlled resonances in nonlinear regimes of motion. The flowchart of the overall approach

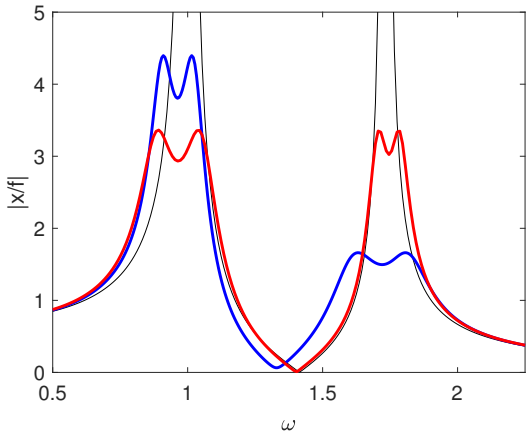

Figure 2: Frequency response function of the host structure (—), solution from [22] (—) and all-equal-peak-design (—).

proposed in this paper, combining the sequential tuning procedures for the linear and nonlinear parameters of the absorbers, is presented in Figure 3.

The equations of motion of the complete system read

$$\mathbf{M}\begin{bmatrix}\ddot{\mathbf{x}}_0\\ \ddot{\mathbf{x}}_a\end{bmatrix}+\mathbf{C}\begin{bmatrix}\dot{\mathbf{x}}_0\\ \dot{\mathbf{x}}_a\end{bmatrix}+\mathbf{K}\begin{bmatrix}\mathbf{x}_0\\ \mathbf{x}_a\end{bmatrix}+\begin{bmatrix}\mathbf{g}_0(\mathbf{x}_0)\\ \mathbf{0}\end{bmatrix}+\begin{bmatrix}\mathbf{B}\mathbf{g}_a(\mathbf{B}^T\mathbf{x}_0-\mathbf{x}_a)\\ -\mathbf{g}_a(\mathbf{B}^T\mathbf{x}_0-\mathbf{x}_a)\end{bmatrix}=\begin{bmatrix}\mathbf{f}\\ \mathbf{0}\end{bmatrix}, \tag{3}$$

where vector $\mathbf{g}_0$ gathers the nonlinearities of the host structure, and $\mathbf{g}_a$ is a vector containing the absorbers nonlinearities. A more convenient form of the equations of motion is obtained through normalization by the forcing amplitude f. Without loss of generality, the nonlinearities are assumed to be polynomials of order $p > 1$. The normalized equations of motion read

$$\mathbf{M}\begin{bmatrix}\ddot{\mathbf{y}}_0\\ \ddot{\mathbf{y}}_a\end{bmatrix}+\mathbf{C}\begin{bmatrix}\dot{\mathbf{y}}_0\\ \dot{\mathbf{y}}_a\end{bmatrix}+\mathbf{K}\begin{bmatrix}\mathbf{y}_0\\ \mathbf{y}_a\end{bmatrix}+\epsilon\begin{bmatrix}\mathbf{g}_0(\mathbf{y}_0)\\ \mathbf{0}\end{bmatrix}+\epsilon\begin{bmatrix}\mathbf{B}\mathbf{g}_a(\mathbf{B}^T\mathbf{y}_0-\mathbf{y}_a)\\ -\mathbf{g}_a(\mathbf{B}^T\mathbf{y}_0-\mathbf{y}_a)\end{bmatrix}=\begin{bmatrix}\mathbf{w}_f\\ \mathbf{0}\end{bmatrix}, \tag{4}$$

in which $\mathbf{y}_0 = \mathbf{x}_0/f$, $\mathbf{w}_f = \mathbf{f}/f$ and $\epsilon = f^{p-1}$.

Similarly to what was achieved for a single NLTVA [16, 17], this work proposes to use a *nonlinear principle of similarity* to ensure that the multiple NLTVAs be effective in a larger range of forcing amplitudes. The polynomial order of the NLTVA nonlinearities is thus the same as the polynomial order of the nonlinearity of the host structure.

3.1. Approximate nonlinear frequency response

The formalism used herein is similar to that used in [23]. Adopting a one-term harmonic balance formalism [24, 25], the vector of generalized degrees of freedom is approximated as

$$\begin{bmatrix}\mathbf{y}_0(t)\\ \mathbf{y}_a(t)\end{bmatrix}=\mathbf{z}_s\sin(\omega t)+\mathbf{z}_c\cos(\omega t),\qquad \mathbf{z}^T=\left[\mathbf{z}_s^T\ ,\ \mathbf{z}_c^T\right]. \tag{5}$$

Inserting Equation (5) into Equation (4) and applying a Galerkin procedure, the following set of algebraic equations is obtained:

$$\mathbf{A}(\omega)\mathbf{z}+\epsilon\mathbf{b}_0(\mathbf{z})+\epsilon\sum_{n=1}^{N_a}b_{a,n}\mathbf{b}_{a,n}(\mathbf{z})=\mathbf{b}_{ext}, \tag{6}$$

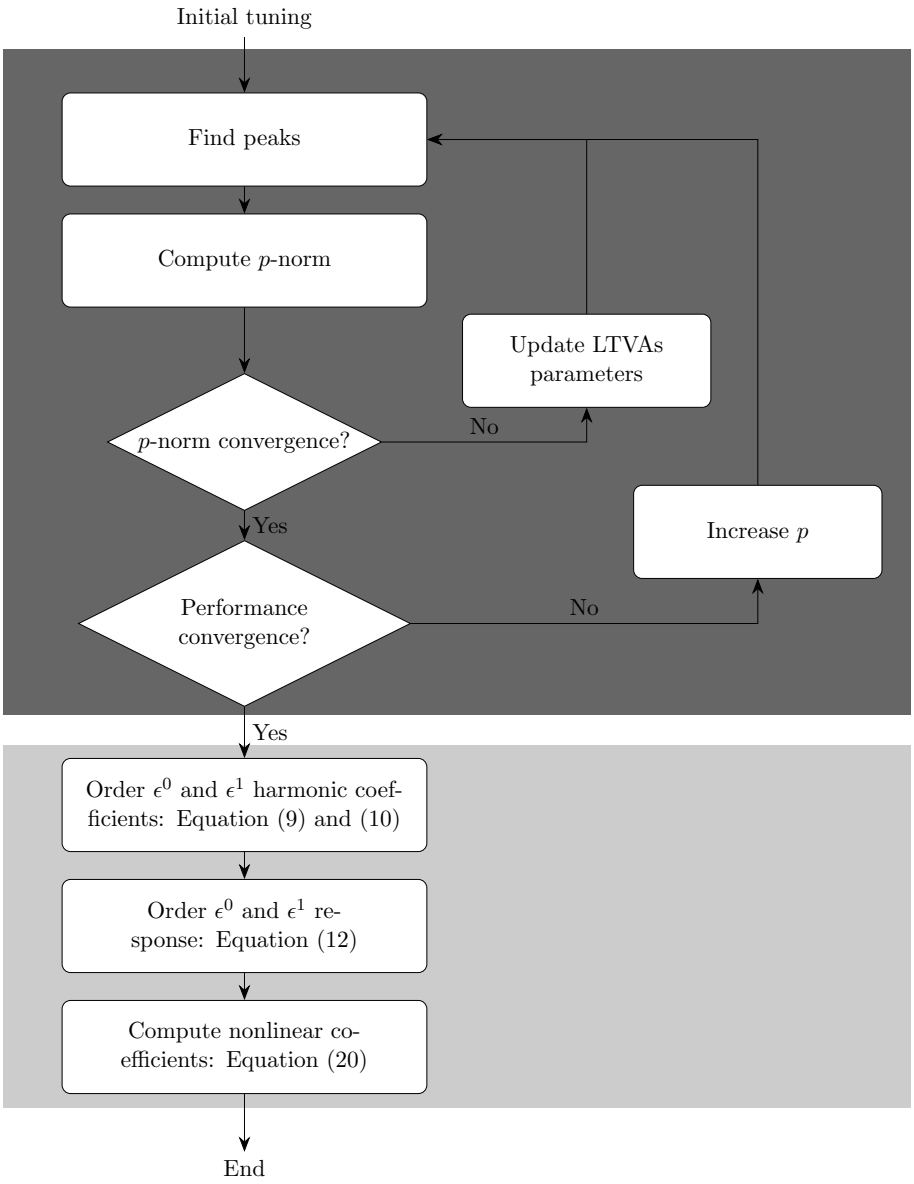

Figure 3: Flowchart of the proposed approach: the dark gray area represents the norm-homotopy optimization [19] and the pale gray area represents the approach detailed in this paper.

in which $\mathbf{A}$ is a matrix representing the linear dynamics of the structure, i.e.,

$$\mathbf{A}(\omega) = \begin{bmatrix} \mathbf{K} - \omega^2\mathbf{M} & -\omega\mathbf{C} \\ \omega\mathbf{C} & \mathbf{K} - \omega^2\mathbf{M} \end{bmatrix}, \tag{7}$$

The vectors $\mathbf{b}$ represent forcing terms with subscripts ext, 0 and a, n corresponding to the external forcing, the nonlinear forces in the host structure, and the nonlinear force in the n^{th} absorber, respectively. $b_{a,n}$ are the associated nonlinear coefficients. These nonlinear terms can be derived analytically or using the alternating frequency-time technique [26].

Equation (6) can be solved numerically. The amplitude of the nonlinear motion can then be

inferred, and optimization algorithms can be used to tune the nonlinear coefficients of the absorbers according to the objectives at hand. Owing to the nonlinear nature of these equations, this process may be time-consuming and end up in a local minimum.

Following the approach in [16], an approximate solution to these equations is derived through a straightforward expansion of the harmonic coefficients in powers of ϵ

$$\mathbf{z} = \sum_{i=0}^{+\infty} \epsilon^i \mathbf{z}^{(i)} \tag{8}$$

Inserting the ansatz (8) into Equation (6) and equating like powers of ϵ leads to a hierarchy of linear equations

$$\mathbf{z}^{(0)} = \mathbf{A}^{-1}\mathbf{b}_{ext}, \tag{9}$$

$$\mathbf{z}^{(1)} = -\mathbf{A}^{-1}\left(\mathbf{b}_0(\mathbf{z}^{(0)}) + \sum_{n=1}^{N_a} b_{a,n}\mathbf{b}_{a,n}(\mathbf{z}^{(0)})\right) = \mathbf{z}_0^{(1)} + \sum_{n=1}^{N_a} b_{a,n}\mathbf{z}_{a,n}^{(1)}. \tag{10}$$

Equation (9) is the exact solution of Equation (6) when $\epsilon = 0$; it expresses that the zeroth-order motion is the response of the underlying linear system. The proposed method may thus be seen as a perturbation method around the equilibrium of the underlying linear structure. Equation (10) shows that the first-order nonlinear motion is due to the nonlinear forces triggered by the zeroth-order motion. Moreover, the contribution from each nonlinearity on this first-order motion can be separated explicitly. Because these two equations are linear, they can readily be solved with standard linear algebra methods.

If the response at a particular degree of freedom localized by $\mathbf{w}_u$ is to be computed, the sine and cosine coefficients associated with it are given by

$$q_s^{(i)} = [\mathbf{w}_u^T, \mathbf{0}]\mathbf{z}^{(i)}, \qquad q_c^{(i)} = [\mathbf{0}, \mathbf{w}_u^T]\mathbf{z}^{(i)}, \tag{11}$$

The squared motion amplitude to first order in ϵ is given by

$$\begin{aligned} H &= \left(q_s^{(0)}\right)^2 + \left(q_c^{(0)}\right)^2 + 2\epsilon\left(q_s^{(0)}q_{s,0}^{(1)} + q_c^{(0)}q_{c,0}^{(1)}\right) + 2\epsilon\sum_{n=1}^{N_a} b_{a,n}\left(q_s^{(0)}q_{s,a,n}^{(1)} + q_c^{(0)}q_{c,a,n}^{(1)}\right) \\ &= H^{(0)} + \epsilon H_0^{(1)} + \epsilon\sum_{n=1}^{N_a} b_{a,n}H_{a,n}^{(1)} \end{aligned}. \tag{12}$$

Equation (12) shows that the effects of the different nonlinearities can once again be separated. In some sense, the nonlinear coefficients of the absorbers can be used to shape the first-order effects of all the nonlinearities on the nonlinear frequency response.

3.2. Enforcing equal peaks in nonlinear regimes of motion

The condition to maintain equal peaks around a specific nonlinear resonance i is

$$H(\hat{\omega}_{i,1}) - H(\hat{\omega}_{i,2}) = 0, \tag{13}$$

where $\hat{\omega}_{i,1}$ and $\hat{\omega}_{i,2}$ are the frequencies of the two resonances appearing around the uncontrolled resonance due to the addition of a NLTVA.

In order to locate both resonances, the necessary condition [16]:

$$\left.\frac{\partial H}{\partial \omega}\right|_{\omega=\hat{\omega}_i} = 0, \tag{14}$$

is considered. The deviation of the nonlinear resonance frequency from its linear counterpart is defined as

$$\Delta\omega_i = \hat{\omega}_i - \omega_i \tag{15}$$

Equation (14) can be doubly expanded as a Maclaurin series in $\Delta\omega_i$ and a power series in ϵ as

$$\left.\frac{\partial H}{\partial \omega}\right|_{\omega=\hat{\omega}_i} = \sum_{k=0}^{+\infty} \frac{(\Delta\omega_i)^k}{k!} \left.\frac{\partial^{k+1} H}{\partial \omega^{k+1}}\right|_{\omega=\omega_i} = \sum_{k=0}^{+\infty} \frac{(\Delta\omega_i)^k}{k!} \left.\left(\sum_{l=0}^{+\infty} \epsilon^l \frac{\partial^{k+1} H^{(l)}}{\partial \omega^{k+1}}\right)\right|_{\omega=\omega_i} = 0 \tag{16}$$

By definition of the linear resonance frequencies and by interpreting $H^{(0)}$ as the linear (squared) FRF, the term corresponding to $(k,l) = (0,0)$ vanishes. The terms corresponding to $(k,l) = (1,0)$ and $(k,l) = (0,1)$ then indicate that $\Delta\omega_i \sim O(\epsilon)$.

The squared amplitude evaluated at the nonlinear resonance frequency is then itself doubly expanded as

$$H|_{\omega=\hat{\omega}_i} = \sum_{k=0}^{+\infty} \frac{(\Delta\omega_i)^k}{k!} \left.\left(\sum_{l=0}^{+\infty} \epsilon^l \frac{\partial^k H^{(l)}}{\partial \omega^k}\right)\right|_{\omega=\omega_i} \tag{17}$$

which becomes, if only terms up to first order in ϵ are considered,

$$H|_{\omega=\hat{\omega}_i} = \left. H^{(0)}\right|_{\omega_i} + \Delta\omega_i \left.\frac{\partial H^{(0)}}{\partial \omega}\right|_{\omega_i} + \epsilon \left. H^{(1)}\right|_{\omega_i} + O\left(\epsilon^2\right) \tag{18}$$

Because the second term in the right hand side of Equation (18) vanishes by definition of the linear resonance frequencies, there is no remaining term depending on $\Delta\omega_i$. Equation (18) thus indicates that, to first order in ϵ, the nonlinear shift of the resonance frequencies has no effect. To impose equal peaks in nonlinear regimes, $\hat{\omega}_{i,1}$ and $\hat{\omega}_{i,2}$ can then be taken as the linear resonance frequencies $\omega_{i,1}$ and $\omega_{i,2}$, respectively.

Combining this result with Equations (12) and (13) yields

$$H^{(0)}(\omega_{i,1}) - H^{(0)}(\omega_{i,2}) + \epsilon \left(H_0^{(1)}(\omega_{i,1}) - H_0^{(1)}(\omega_{i,2}) + \sum_{n=1}^{N_a} b_{a,n} \left(H_{a,n}^{(1)}(\omega_{i,1}) - H_{a,n}^{(1)}(\omega_{i,2}) \right) \right) = 0 \tag{19}$$

Since the linear FRF already exhibits equal peaks (see Section 2), the first two terms in Equation (19) cancel out. Equation (19) then becomes independent of ϵ, which sets one condition on the nonlinear coefficients. Enforcing Equation (19) for each controlled resonance $i = 1, ..., N_a$, one eventually obtains the linear system of equations

$$\begin{bmatrix} \Delta_1 H_1^{(1)} & \Delta_1 H_2^{(1)} & \cdots & \Delta_1 H_{N_a}^{(1)} \\ \Delta_2 H_1^{(1)} & \Delta_2 H_2^{(1)} & \cdots & \Delta_2 H_{N_a}^{(1)} \\ \vdots & \vdots & \ddots & \vdots \\ \Delta_{N_a} H_1^{(1)} & \Delta_{N_a} H_2^{(1)} & \cdots & \Delta_{N_a} H_{N_a}^{(1)} \end{bmatrix} \begin{bmatrix} b_{a,1} \\ \vdots \\ b_{a,N_a} \end{bmatrix} = - \begin{bmatrix} \Delta_1 H_0^{(1)} \\ \vdots \\ \Delta_{N_a} H_0^{(1)} \end{bmatrix} \tag{20}$$

with the shorthand notation

$$\Delta_i H_l^{(1)} = H_l^{(1)}(\omega_{i,1}) - H_l^{(1)}(\omega_{i,2}) \tag{21}$$

The system (20) can be solved to find the nonlinear coefficients that impose equal peaks for all controlled nonlinear resonances. This equation, which is the core result of the present work, allows to find the nonlinear coefficients explicitly, i.e., without resorting to numerical optimization. A graphical interpretation of the counterbalancing action of the NLTVA nonlinearities is displayed in Figure 4.

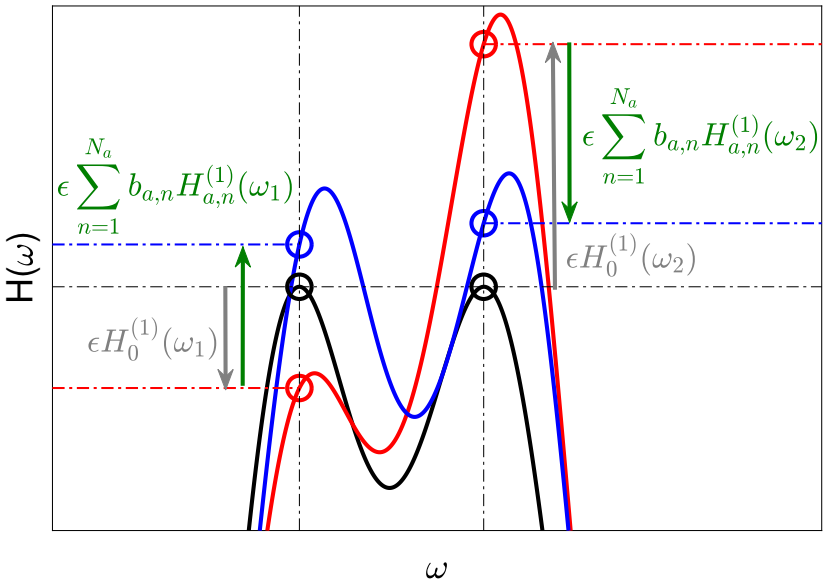

Figure 4: Action of the NLTVA nonlinearities on the frequency response: underlying linear structure $H^{(0)}$ (—), nonlinear structure with linear absorbers (—) and nonlinear structure with nonlinear absorbers. (—)

The assumption of equality of the peaks amplitude in the linear FRF can be relaxed. Indeed, Equation (20) can be interpreted as requiring a cancelling nonlinear action of the absorbers on the imbalance brought by the nonlinearities of the host structure, to first order. Approximately equal peaks in the linear regime will therefore remain approximately equal in nonlinear regimes.

4. Performance of the Multiple Nonlinear Tuned Vibration Absorbers

The proposed approach is illustrated with two spring-mass systems. The nonlinear frequency responses (NFR) of these systems were computed using pseudo-arc length continuation coupled with harmonic balance. This method transforms the system of nonlinear ordinary differential equations (3) into a system of algebraic equations by assuming that the structural response is composed of a sum of harmonics of the fundamental excitation frequency (here, five harmonics are considered). These nonlinear algebraic equations can then be solved using standard Newton-Raphson methods, and the solution found at one frequency can be continued to find the complete NFR within a given frequency bandwidth. More details about this method can be found in [24, 25].

4.1. Two-degree-of-freedom system

The system in Figure 5 is identical to that shown in Figure 1 with an added cubic grounded spring. All mass and stiffness parameters of the host structure are equal to 1, and the nonlinear coefficient is set to 1 (this example is inspired from the literature [27]). Modal damping of 0.05% is added to the two modes. Two NLTVAs are attached, i.e., the first (second) absorber is attached to the second (first) mass and targets the first (second) mode. Their total mass should not exceed 5% of that of the host structure. The linear and nonlinear parameters in Table 1 were computed with the methodology presented in Figure 3.

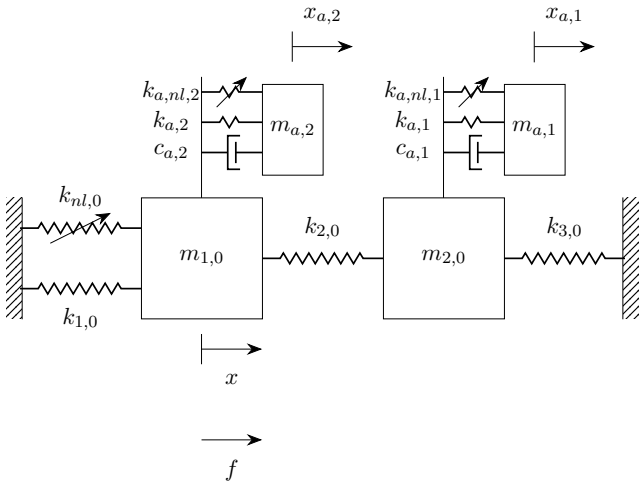

Figure 5: Two-degree-of-freedom system with two NLTVAs.

Parameter	$m_{a,1}$	$m_{a,2}$	$c_{a,1}$	$c_{a,2}$	$k_{a,1}$	$k_{a,2}$	$k_{a,nl,1}$	$k_{a,nl,2}$
Value	0.0971	0.0029	0.0263	0.0003	0.0908	0.0089	0.0046	4.74e-06

Table 1: Parameters of the two NLTVAs.

Figure 6 compares the NFRs of the controlled structure with or without nonlinearities in the absorbers. For low forcing amplitudes, the controlled structure behaves essentially linearly; an all-equal-peak design is achieved. At $f = 0.1$, the cubic nonlinearity of the host structure is responsible for a frequency shift of 23% and 48% of the first two resonance frequencies, respectively; a strongly nonlinear regime of motion is thus considered. This is why the two linear absorbers become detuned. Conversely, because the two nonlinear absorbers are able to track the increase in resonance frequency shift, a pair of equal peaks can be maintained for each resonance. However, we note that the all-equal-peak design is now lost; the two pairs of equal peaks have no longer the same amplitude.

To assess the accuracy of the analytical developments, the NFRs for various scaled nonlinear coefficients were calculated numerically. Figure 7 confirms that the nonlinear coefficients provided by the analytical design (black curve) are those which enforce equal peaks in the best manner. We note that these loci of resonance peaks were computed following the method presented in [28].

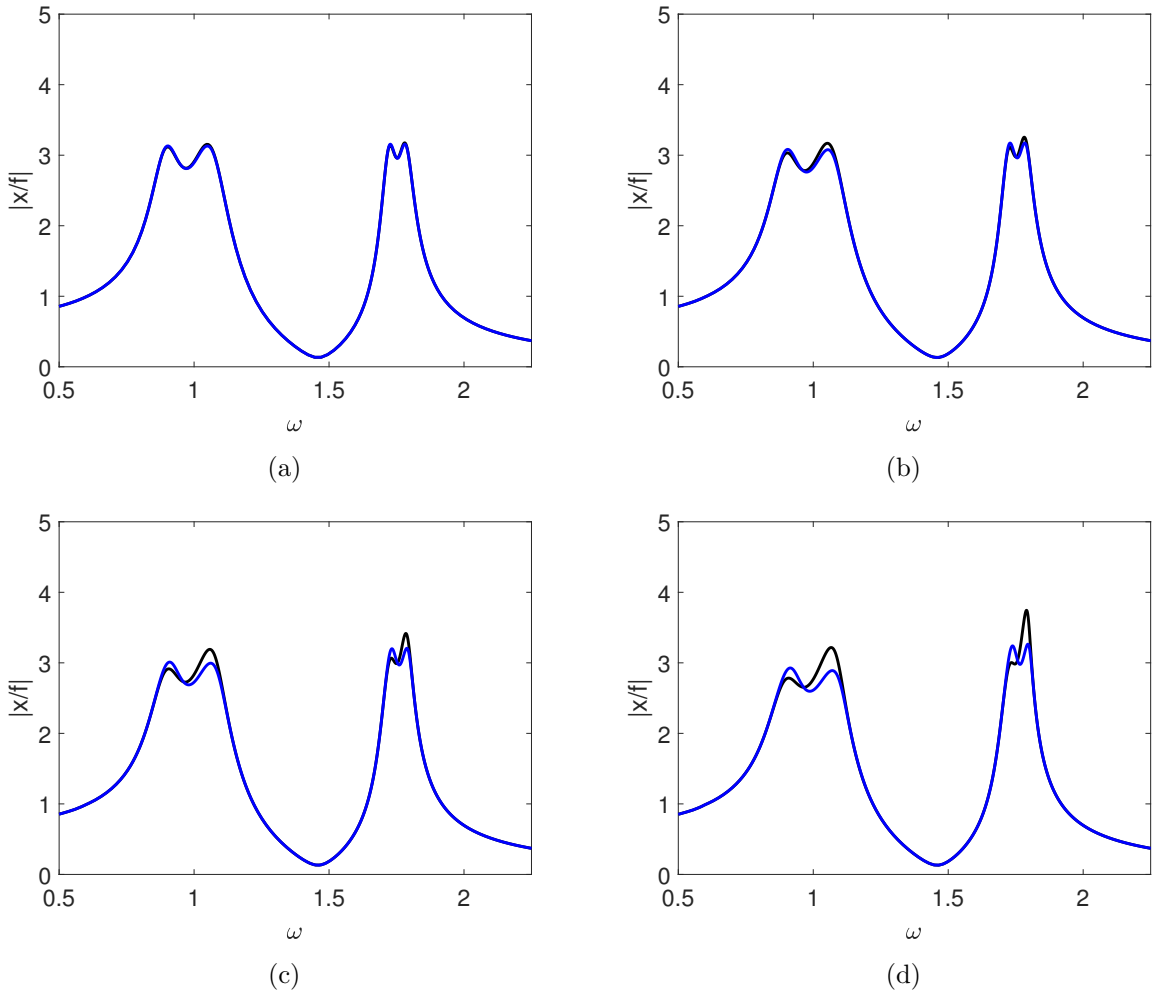

Figure 6: NFRs with linear (—) and nonlinear (—) absorbers: f =0.025 (a), f =0.05 (b), f =0.075 (c) and f =0.1 (d).

4.1.1. Detached resonance curve

The higher-order terms omitted in Equation (12) may become significant for large ϵ. Figure 8, which shows the NFRs at larger forcing levels, reveals the existence of a detached resonance curve (DRC). This DRC grows until it merges with the second resonance of the main NFR. The DRC appearance seems to be independent of whether or not nonlinearities are present in the absorbers, as seen in Figure 8 (a), but the nonlinear absorbers delay its merging with the main NFR in Figure 8 (b)-(c). For $f = 0.18$, the DRC has coalesced with the main NFR for the two types of absorbers. Another view of this process is given in Figure 9. We note that a similar trend was observed with a single NLTVA [18]. Discontinued curves appear in Figure 9 owing to the disappearance of a peak when merging with a local minimum at some forcing amplitude, thereby resulting in an NFR with a single peak instead of two (as can also be observed in Figures 8 (c)-(d)) for the LTVAs.

Further insight on the system behavior can be gained by looking at the absorbers responses. Figures 10 and 11 display the NFRs of the first and second absorber, respectively. As seen in

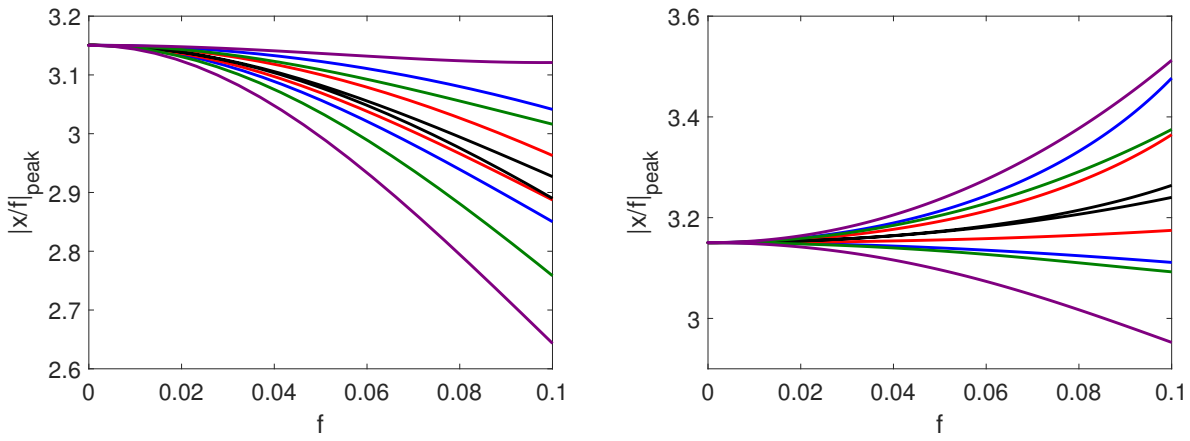

(a) (b)

Figure 7: Loci of resonant peaks with nonlinear absorbers near the first mode when $k_{a,nl,1}$ is multiplied by a scaling factor (a) and near the second mode when $k_{a,nl,2}$ is multiplied by a scaling factor (b). Scaling factors: 0.5 (—), 0.75 (—), 1 (—), 1.5 (—) and 2 (—).

Figure 10, the first absorber is mostly active near the first mode of the host structure, thereby evidencing its vibration mitigation ability. Similarly, Figure 11 indicates that the nominal working mechanism of the second absorber is to be active near the second mode. However, a DRC coexists with the main NFR, where the absorber loses effectiveness, thus enabling high-amplitude vibrations of the host structure. As in Figure 8, Figure 11 indicates that the NLTVAs are not able to suppress this DRC but are able to delay its coalescence with the main NFR.

To investigate whether a DRC is also present near the first mode, basins of attraction were computed through numerical integration of Equation (3) under harmonic forcing. Based on the linear mode shapes of the host structure, various initial positions and velocities were considered for the two main masses with the absorbers at rest. Figure 12 confirms the existence of the DRC in the vicinity of the second mode, but no such attractor was found for the first mode.

4.1.2. Quasiperiodic oscillations

Figure 8 also features Neimark-Sacker (NS) bifurcations which are at the onset of quasiperiodic (QP) oscillations. QP responses cannot be assessed with classical harmonic balance because the motion is no longer periodic, but we computed them using the method proposed in [29]. This method extends the traditional harmonic balance method by assuming a multi-frequency, multi-harmonic structural response. When an NS bifurcation is found by the traditional harmonic balance [24, 25], the emanating branch of QP solution is found using the nonlinear unstable mode associated with the pair of Floquet exponents crossing the imaginary axis, characteristics of NS bifurcations [29, 30]. Five and twenty-five harmonics were used for the forcing frequency and the second frequency, respectively.

Stability was assessed with the method proposed in [31]. In this method, the monodromy matrix is obtained through time-integration of the equations of motion (Equation (6)) linearized around the computed equilibrium. This matrix is interpolated over a first-order stroboscopic section (defined as the set of points in state space such that $t = k2\pi/\omega$, $k \in \mathbb{Z}$) to approximate its value on a second-order stroboscopic section (defined as the intersection between the aforemen-

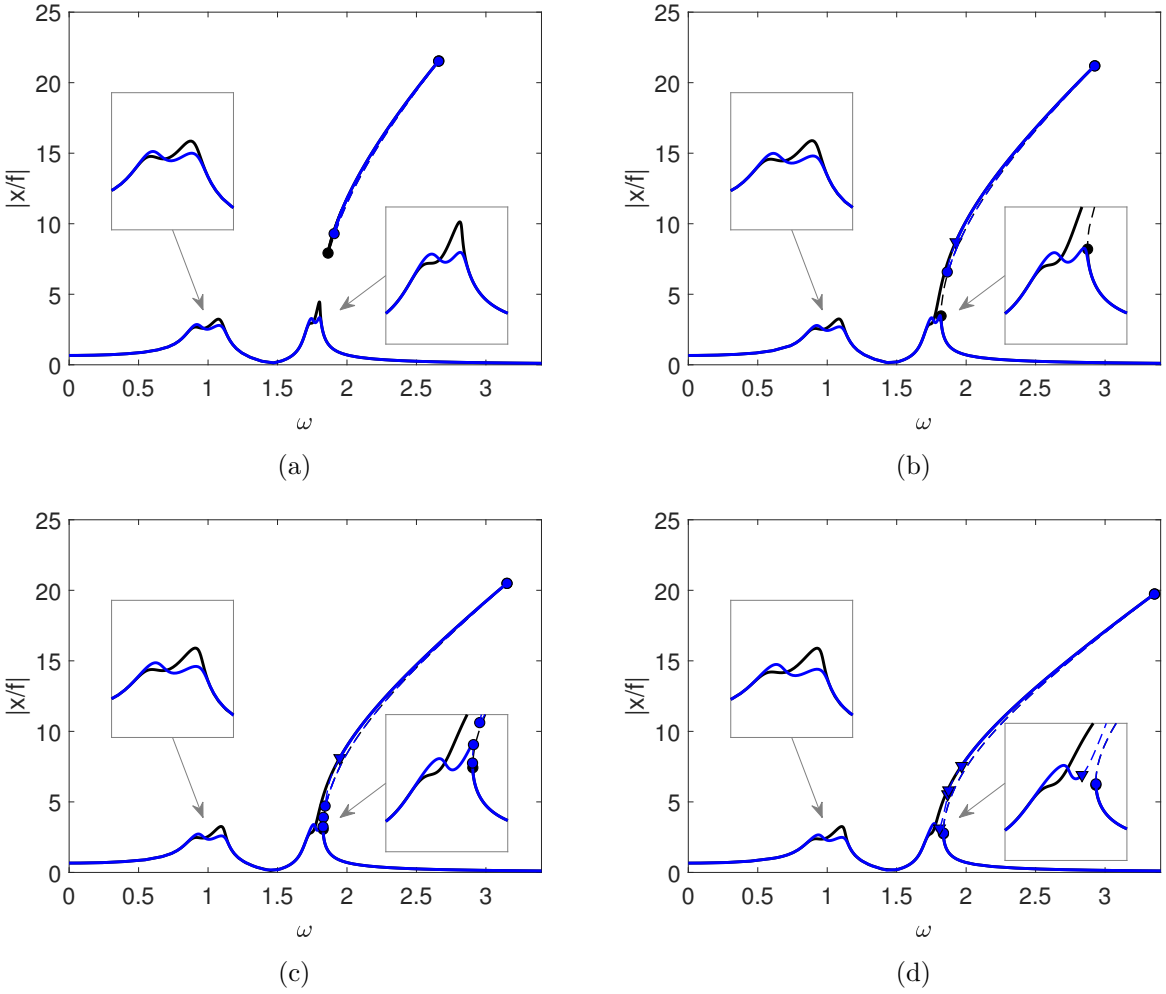

Figure 8: NFRs with linear (—) and nonlinear (—) absorbers: f =0.12 (a), f =0.14 (b), f =0.16 (c) and f =0.18 (d). —: stable solution, - - : unstable solution, •: fold bifurcation, ▼: Neimark-Sacker bifurcation.

tioned first-order section and another one characterized by $t = k2\pi/\omega_2$, $k \in \mathbb{Z}$, where ω_2 is the additional frequency present in the QP motion). The eigenvalues of this matrix are then taken as approximations of the Floquet multipliers, providing information on the stability of the computed solution.

The QP regime exhibits a more complicated frequency response than the harmonic one, as displayed in Figure 13. A forcing amplitude $f = 0.165$ was considered, i.e., slightly after the DRC coalescence with the main NFR. Two branches emanate from the NS bifurcations but do not join. These two branches are only partially stable, and both lose stability through fold bifurcations. Thus, the DRC does not seem to be connected to the main NFR by any fully stable branch. Other solutions were obtained through direct time integration of Equation (3) with initial conditions such that the motion initially lies on the computed QP branches. They are superimposed with the NFR in Figure 13 and fully agree with it. At the apparent end of either QP branch, the second frequency ω_2 is zero; the continuation procedure turns back toward negative ω_2. A branch projected on the frequency-amplitude plane appears fully folded on itself, and does not really end where it appears

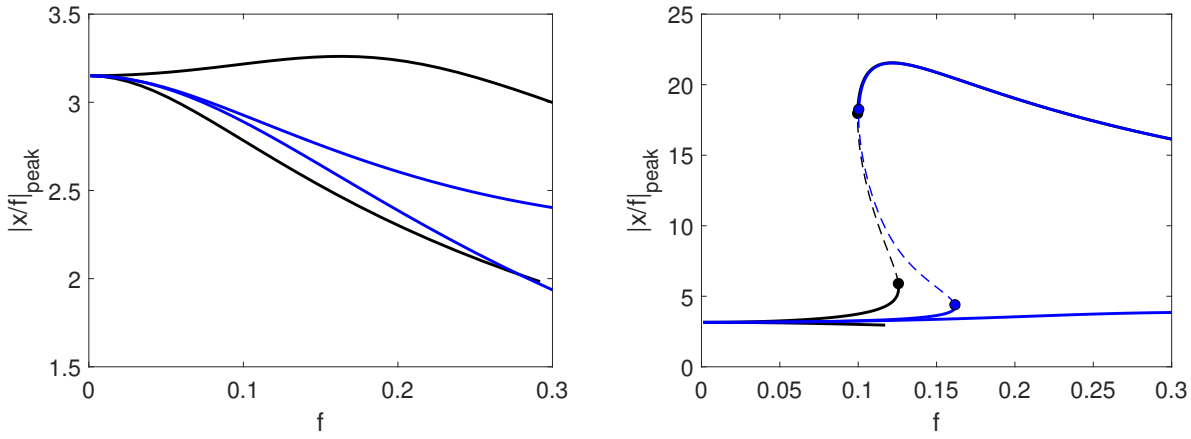

(a) (b)

Figure 9: Loci of resonant peaks with linear (—) and nonlinear (—) absorbers near the first (a) and second (b) resonance. —: stable solution, - - : unstable solution, •: fold bifurcation

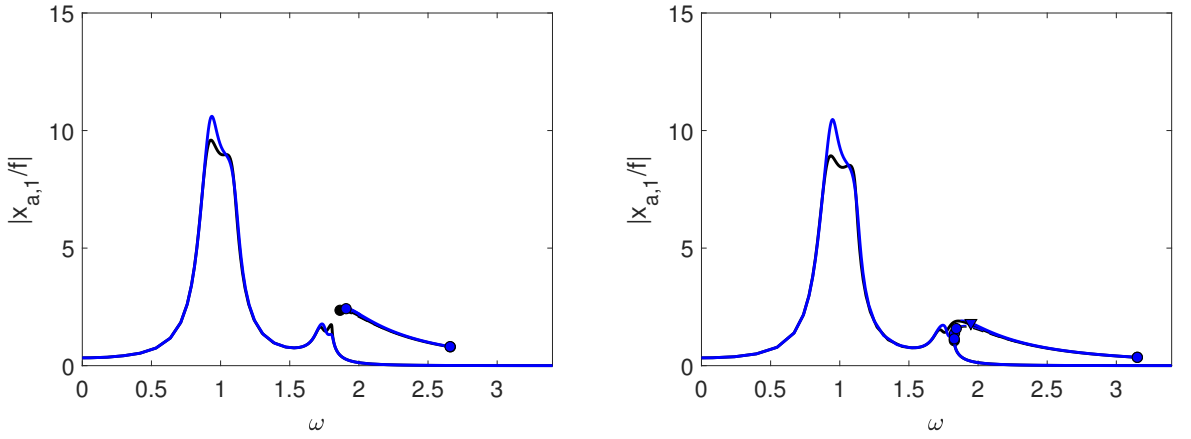

(a) (b)

Figure 10: NFRs of the first absorber with linear (—) and nonlinear (—) absorbers: f =0.12 (a) and f =0.16 (b). —: stable solution, - - : unstable solution, •: fold bifurcation, ▼: Neimark-Sacker bifurcation.

to.

4.2. Five-degree-of-freedom system

The system inspired from [23] is depicted in Figure 14. All masses are equal to 1, and all linear springs have unit stiffness except $k_{1,0} = 1.5$ and $k_{3,0} = 0.2$. A cubic spring with unit coefficient connects the first mass to ground. Modal damping of 0.1% is added to all modes, whose frequencies are listed in Table 2.

Two configurations were studied, where two NLTVAs control a pair of modes, namely modes 1 and 2, and then modes 2 and 4. The subscripts in the absorber parameters in Figure 14 refer to the mode they are tuned to. The maximum mass allowed for the absorbers is 3% of that of the host structure. The absorber parameters are listed in Tables 3 and 4, respectively.

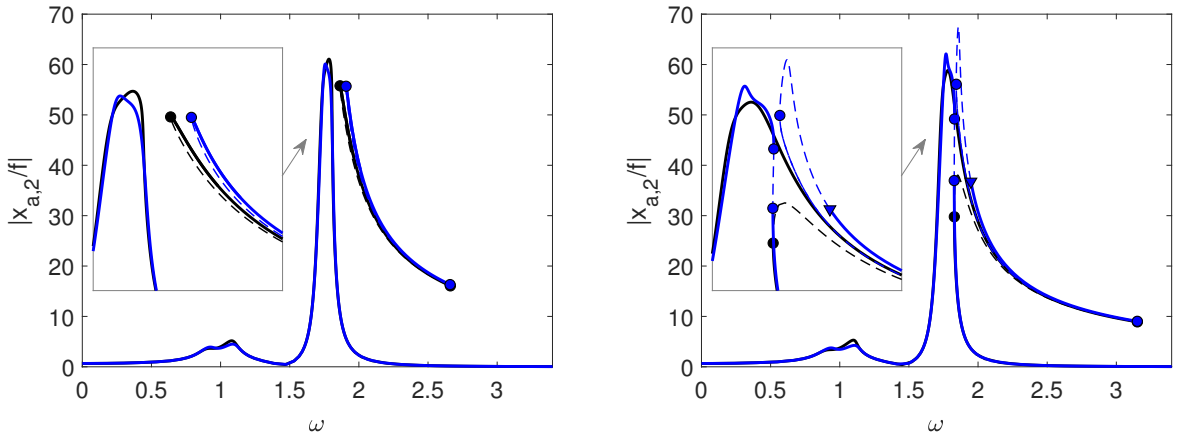

Figure 11: NFRs of the second absorber with linear (—) and nonlinear (—) absorbers: f =0.12 (a) and f =0.16 (b). —: stable solution, - - : unstable solution, •: fold bifurcation, ▼: Neimark-Sacker bifurcation.

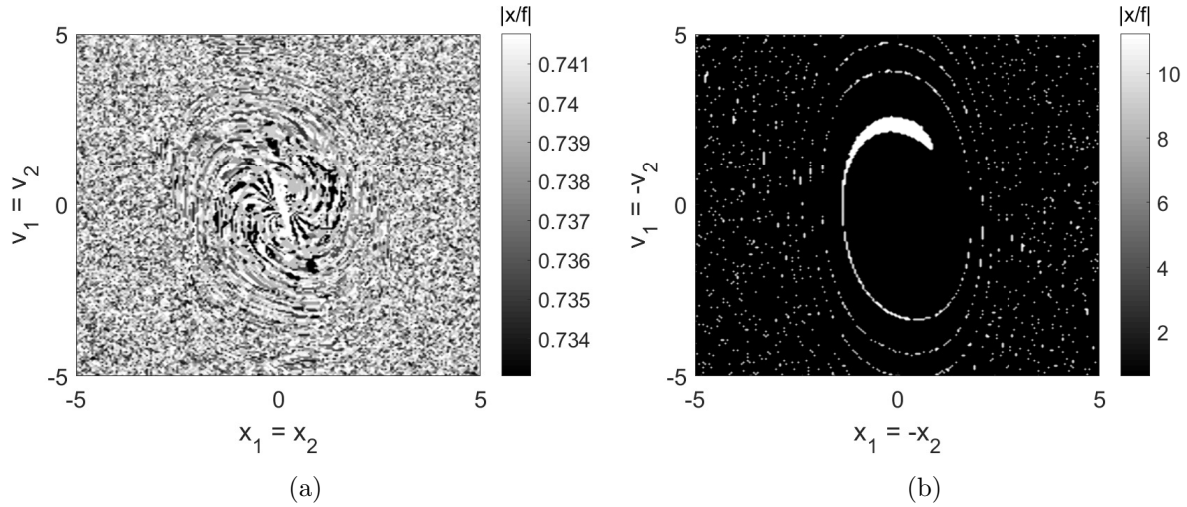

Figure 12: Basins of attraction at f=0.125: ω=1.25 (a) and ω=2 (b). $x_{1,2}$ and $v_{1,2}$ are the initial displacement and velocity of the first and second mass, respectively.

Frequency (rad/s)	ω_1	ω_2	ω_3	ω_4	ω_5
Value	0.51	0.83	1.28	1.74	1.81

Table 2: Linear natural frequencies of five-degree-of-freedom system.

Parameter	$m_{a,1}$	$m_{a,2}$	$c_{a,1}$	$c_{a,2}$	$k_{a,1}$	$k_{a,2}$	$k_{a,nl,1}$	$k_{a,nl,2}$
Value	0.0155	0.1345	0.0008	0.0357	0.0038	0.0772	1.95×10^{-7}	0.0011

Table 3: Absorber parameters for the control of modes 1 and 2 ($m_{a,4} = 0$).

Figure 15 (a) shows that the two NLTVAs can maintain equal peaks for modes 1 and 2 for the

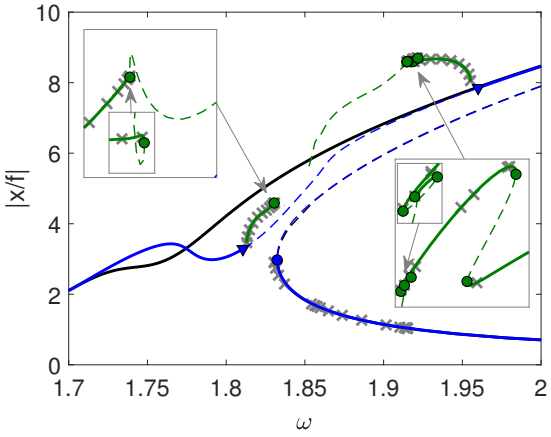

Figure 13: Close-up of the NFR at f =0.165 with linear (—) and nonlinear (—: periodic motion, —: QP motion, ×: time integration results) absorbers. —: stable solution, - - : unstable solution, •: fold bifurcation, ▼: Neimark-Sacker bifurcation.

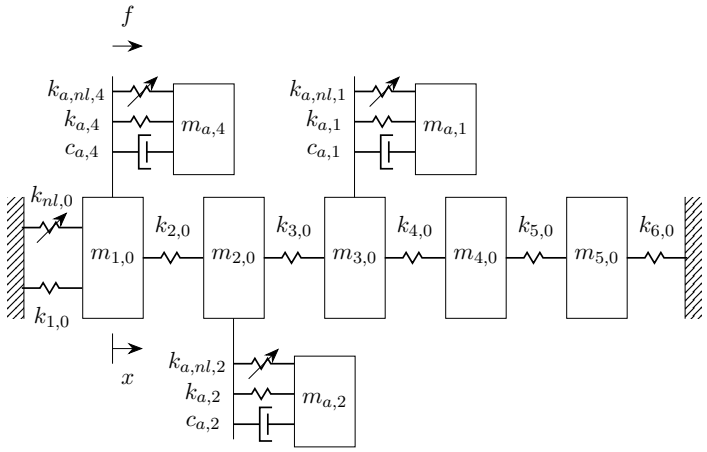

Figure 14: Five-degree-of-freedom system with three NLTVAs.

Parameter	$m_{a,2}$	$m_{a,4}$	$c_{a,2}$	$c_{a,4}$	$k_{a,2}$	$k_{a,4}$	$k_{a,nl,2}$	$k_{a,nl,4}$
Value	0.1038	0.0462	0.0248	0.0174	0.0612	0.1338	0.0007	0.002

Table 4: Absorber parameters for the control of modes 2 and 4 ($m_{a,1} = 0$).

three forcing amplitudes considered. The effectiveness of the NLTVAs for modes 2 and 4 is also confirmed in Figure 15 (b).

4.2.1. Influence of internal resonances

The one-term harmonic balance approximation made in Subsection 3.1 may overlook possible internal resonances (other than 1:1) [24], which may limit the absorbers performance. To investigate this, a second set of parameters is now considered, i.e., $k_{1,0} = 1$ and $k_{3,0} = 0.1$. The computed absorber parameters for the control of modes 1 and 2 are given in Table 5. Although the mitigation performance is still satisfactory, Figure 16 (a) depicts that equal peaks for mode 2 cannot be

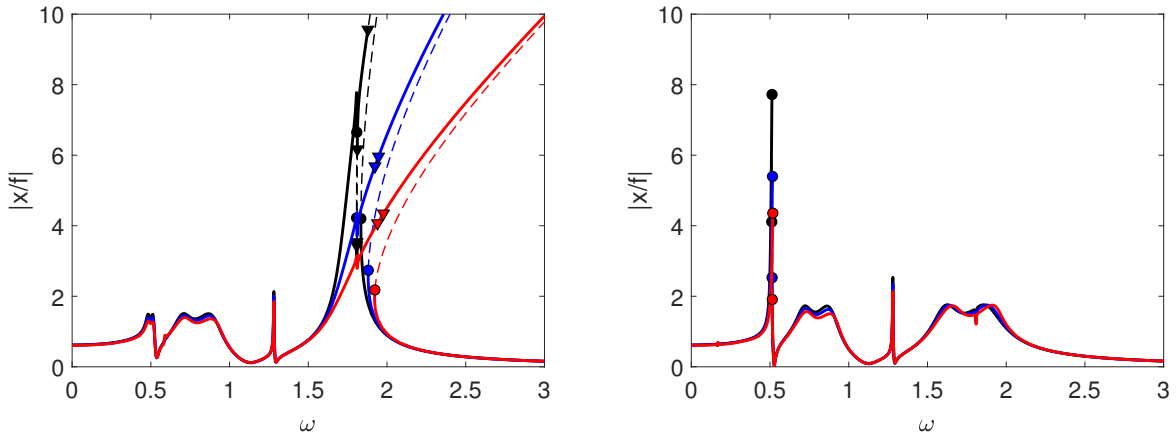

Figure 15: NFR for configuration 1 (a) and configuration 2 (b): f=0.1 (—), f=0.2 (—) and f=0.3 (—). (—: stable solution, - - : unstable solution, •: fold bifurcation, ▼: Neimark-Sacker bifurcation).

enforced. The reason for this failure can be understood from Figure 16 (b), i.e., a 3:1 superharmonic resonance with mode 4 occurs at a frequency near that of the second mode. This failure is a direct consequence of Equation (5), which does not account for the third harmonic. Thus, sub- or superharmonic resonances of uncontrolled modes may limit the performance of the absorbers tuned with the proposed approach. Within the range of its approximations however, the method remains successful as the peaks of the fundamental harmonic remain approximately equal.

Characteristic	$m_{a,1}$	$m_{a,2}$	$c_{a,1}$	$c_{a,2}$	$k_{a,1}$	$k_{a,2}$	$k_{a,nl,1}$	$k_{a,nl,2}$
Value	0.0096	0.1404	0.0004	0.0308	0.0021	0.0561	1.67×10^{-7}	0.002

Table 5: Absorber parameters for the control of modes 1 and 2 of the modified host ($m_{a,4} = 0$).

5. Conclusion

This paper presented a tuning methodology for multiple nonlinear vibration absorbers that mitigate several nonlinear resonances simultaneously. The nonlinear absorbers were shown to be able to maintain equal peaks in the frequency response over a broader range of forcing amplitudes than their linear counterparts.

Adverse attractors, including detached resonance curves, quasiperiodic responses and superharmonic resonances, were studied, highlighting that the coupled system can exhibit complex and potentially detrimental dynamics. However, these attractors were observed whether or not nonlinearities were used in the absorbers. We can therefore conclude that the performance of the developed nonlinear absorbers is always superior to that of linear absorbers.

Future works may involve the experimental validation of the proposed approach, and its extension to multiple harmonics to overcome the limitations due to internal resonances.

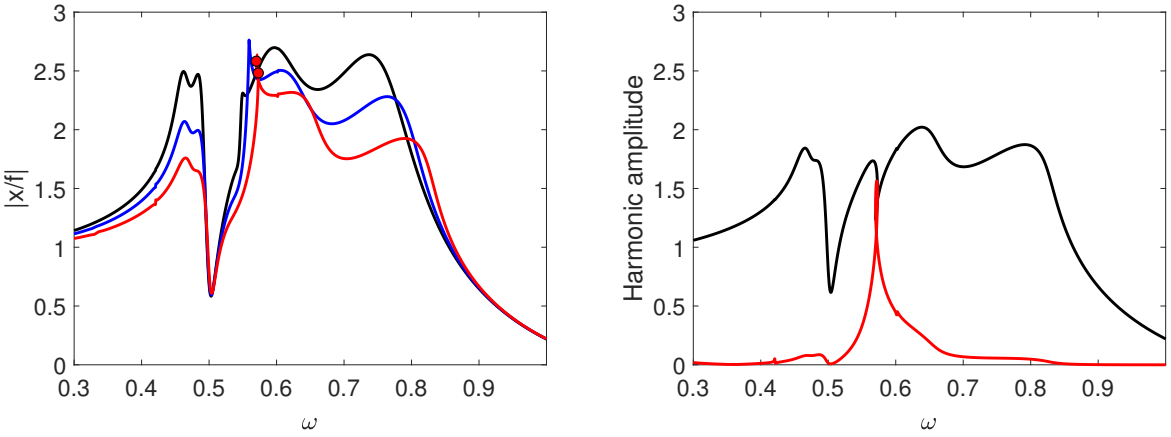

(a) (b)

Figure 16: NFRs (a) (—: stable solution, - - : unstable solution, •: fold bifurcation) of the first configuration, with a modified host structure: f=0.1 (—), f=0.2 (—) and f=0.3 (—); harmonics amplitudes (b) (—: first harmonic, —: third harmonic) at f=0.3.

Acknowledgements

The authors would like to acknowledge the financial support of the SPW (WALInnov grant 1610122).

[1] H. Frahm, Device for Damping Vibrations of Bodies (1911).

[2] J. Den Hartog, J. Ormondroyd, Theory of the dynamic vibration absorber, Journal of Applied Mechanics 50 (7) (1928) 11–22.

[3] J. E. Brock, A Note on the Damped Vibration Absorber, Transactions of the ASME, Journal of Applied Mechanics 13 (4) (1946) A–284.

[4] O. Nishihara, T. Asami, Closed-Form Solutions to the Exact Optimizations of Dynamic Vibration Absorbers (Minimizations of the Maximum Amplitude Magnification Factors), Journal of Vibration and Acoustics 124 (4) (2002) 576. doi:10.1115/1.1500335.
URL http://vibrationacoustics.asmedigitalcollection.asme.org/article.aspx?articleid=1470453

[5] O. Gendelman, L. I. Manevitch, A. F. Vakakis, R. M'Closkey, Energy Pumping in Nonlinear Mechanical Oscillators: Part IDynamics of the Underlying Hamiltonian Systems, Journal of Applied Mechanics 68 (1) (2001) 34. doi:10.1115/1.1345524.
URL http://appliedmechanics.asmedigitalcollection.asme.org/article.aspx?articleid=1555314

[6] A. F. Vakakis, O. Gendelman, Energy Pumping in Nonlinear Mechanical Oscillators: Part IIResonance Capture, Journal of Applied Mechanics 68 (1) (2001) 42. doi:10.1115/1.1345525.
URL http://appliedmechanics.asmedigitalcollection.asme.org/article.aspx?articleid=1555315http://www.intangiblecapital.org/index.php/ic/article/view/911

[7] F. Petit, M. Loccufier, D. Aeyels, The energy thresholds of nonlinear vibration absorbers, Nonlinear Dynamics 74 (3) (2013) 755–767. doi:10.1007/s11071-013-1003-8.
URL http://link.springer.com/10.1007/s11071-013-1003-8

[8] G. Habib, F. Romeo, The tuned bistable nonlinear energy sink, Nonlinear Dynamics 89 (1) (2017) 179–196. doi:10.1007/s11071-017-3444-y.
URL http://link.springer.com/10.1007/s11071-017-3444-y

[9] G. S. Agnes, Performance of Nonlinear Mechanical , Resonant-Shunted Piezoelectric , and Electronic Vibration Absorbers for Multi-Degree-of-Freedom Structures, Ph.D. thesis, Virginia Polytechnic Institute and State University in (1997).

[10] B. Balachandran, Y. Y. Li, C. C. Fang, A mechanical filter concept for control of non-linear crane-load oscillations, Journal of Sound and Vibration 228 (3) (1999) 651–682. doi:10.1006/jsvi.1999.2440.
URL https://linkinghub.elsevier.com/retrieve/pii/S0022460X99924409

[11] V. Gattulli, F. Di Fabio, A. Luongo, Nonlinear Tuned Mass Damper for self-excited oscillations, Wind and Structures 7 (4) (2004) 251–264. doi:10.12989/was.2004.7.4.251.
URL http://koreascience.or.kr/journal/view.jsp?kj=KJKHCF{&}py=2004{&}vnc=v7n4{&}sp=251

[12] M. Yaman, S. Sen, The analysis of the orientation effect of non-linear flexible systems on performance of the pendulum absorber, International Journal of Non-Linear Mechanics 39 (5) (2004) 741–752. doi:10.1016/S0020-7462(03)00038-6.
URL https://linkinghub.elsevier.com/retrieve/pii/S0020746203000386

[13] B. Vazquez-Gonzalez, G. Silva-Navarro, Evaluation of the Autoparametric Pendulum Vibration Absorber for a Duffing System, Shock and Vibration 15 (3-4) (2008) 355–368. doi:10.1155/2008/827129.
URL http://www.hindawi.com/journals/sv/2008/827129/

[14] H. Jo, H. Yabuno, Amplitude reduction of primary resonance of nonlinear oscillator by a dynamic vibration absorber using nonlinear coupling, Nonlinear Dynamics 55 (1-2) (2009) 67–78. doi:10.1007/s11071-008-9345-3.
URL http://link.springer.com/10.1007/s11071-008-9345-3

[15] R. Viguié, G. Kerschen, Nonlinear vibration absorber coupled to a nonlinear primary system: A tuning methodology, Journal of Sound and Vibration 326 (3-5) (2009) 780–793. doi:10.1016/j.jsv.2009.05.023.
URL https://linkinghub.elsevier.com/retrieve/pii/S0022460X09004490

[16] G. Habib, G. Kerschen, A principle of similarity for nonlinear vibration absorbers, Physica D: Nonlinear Phenomena 332 (2016) 1–8. arXiv:1606.01244, doi:10.1016/j.physd.2016.06.001.
URL http://dx.doi.org/10.1016/j.physd.2016.06.001https://linkinghub.elsevier.com/retrieve/pii/S0167278915300580

[17] G. Habib, T. Detroux, R. Viguié, G. Kerschen, Nonlinear generalization of Den Hartog's equal-peak method, Mechanical Systems and Signal Processing 52-53 (1) (2015) 17–28. arXiv:arXiv:1604.03868v1, doi:10.1016/j.ymssp.2014.08.009.
URL http://dx.doi.org/10.1016/j.ymssp.2014.08.009

[18] T. Detroux, G. Habib, L. Masset, G. Kerschen, Performance, robustness and sensitivity analysis of the nonlinear tuned vibration absorber, Mechanical Systems and Signal Processing 60 (2015) 799–809. arXiv:arXiv:1604.05524v1, doi:10.1016/j.ymssp.2015.01.035.
URL http://dx.doi.org/10.1016/j.ymssp.2015.01.035

[19] G. Raze, G. Kerschen, All-equal-peak design of multiple tuned mass dampers using norm-homotopy optimizationarXiv:1905.03574.
URL http://arxiv.org/abs/1905.03574

[20] G. Kerschen, J. J. Kowtko, D. M. Mcfarland, L. A. Bergman, A. F. Vakakis, Theoretical and Experimental Study of Multimodal Targeted Energy Transfer in a System of Coupled Oscillators, Nonlinear Dynamics 47 (1-3) (2006) 285–309. doi:10.1007/s11071-006-9073-5.
URL http://link.springer.com/10.1007/s11071-006-9073-5

[21] K. Dekemele, R. De Keyser, M. Loccufier, Performance measures for targeted energy transfer and resonance capture cascading in nonlinear energy sinks, Nonlinear Dynamics 93 (2) (2018) 259–284. doi:10.1007/s11071-018-4190-5.
URL https://doi.org/10.1007/s11071-018-4190-5

[22] H. Özgüven, B. Çandir, Suppressing the first and second resonances of beams by dynamic vibration absorbers, Journal of Sound and Vibration 111 (3) (1986) 377–390. doi:10.1016/S0022-460X(86)81399-2.
URL https://linkinghub.elsevier.com/retrieve/pii/S0022460X86813992

[23] G. Habib, G. Kerschen, Linearization of nonlinear resonances: Isochronicity and force-displacement proportionality, Journal of Sound and Vibration 457 (2019) 227–239. doi:10.1016/j.jsv.2019.06.007.
URL https://linkinghub.elsevier.com/retrieve/pii/S0022460X1930344X

[24] A. H. Nayfeh, B. Balachandran, Applied Nonlinear Dynamics, Wiley, 1995. doi:10.1002/9783527617548.
URL https://onlinelibrary.wiley.com/doi/book/10.1002/9783527617548

[25] T. Detroux, L. Renson, L. Masset, G. Kerschen, The harmonic balance method for bifurcation analysis of large-scale nonlinear mechanical systems, Computer Methods in Applied Mechanics and Engineering 296 (2015) 18–38. arXiv:1604.05621, doi:10.1016/j.cma.2015.07.017.
URL http://dx.doi.org/10.1016/j.cma.2015.07.017https://linkinghub.elsevier.com/retrieve/pii/S0045782515002297

[26] T. M. Cameron, J. H. Griffin, An Alternating Frequency/Time Domain Method for Calculating the Steady-State Response of Nonlinear Dynamic Systems, Journal of Applied Mechanics 56 (1) (1989) 149. doi:10.1115/1.3176036.
URL http://appliedmechanics.asmedigitalcollection.asme.org/article.aspx?articleid=1409535

[27] M. Peeters, R. Viguié, G. Sérandour, G. Kerschen, J.-C. Golinval, Nonlinear normal modes, Part II: Toward a practical computation using numerical continuation techniques, Mechanical Systems and Signal Processing 23 (1) (2009) 195–216. doi:10.1016/j.ymssp.2008.04.003.
URL https://linkinghub.elsevier.com/retrieve/pii/S0888327008001027

[28] A. Renault, O. Thomas, H. Mahé, Numerical antiresonance continuation of structural systems, Mechanical Systems and Signal Processing 116 (2019) 963–984. doi:10.1016/j.ymssp.2018.07.005.
URL https://doi.org/10.1016/j.ymssp.2018.07.005https://linkinghub.elsevier.com/retrieve/pii/S0888327018304060

[29] B. Zhou, F. Thouverez, D. Lenoir, A variable-coefficient harmonic balance method for the prediction of quasi-periodic response in nonlinear systems, Mechanical Systems and Signal Processing 64-65 (2015) 233–244. doi:10.1016/j.ymssp.2015.04.022.
URL http://dx.doi.org/10.1016/j.ymssp.2015.04.022

[30] J.-J. Sinou, F. Thouverez, L. Jezequel, Stability analysis and non-linear behaviour of structural systems using the complex non-linear modal analysis (CNLMA), Computers & Structures 84 (29-30) (2006) 1891–1905. doi:10.1016/j.compstruc.2006.08.020.
URL https://linkinghub.elsevier.com/retrieve/pii/S0045794906002501

[31] M. Guskov, F. Thouverez, Harmonic Balance-Based Approach for Quasi-Periodic Motions and Stability Analysis, Journal of Vibration and Acoustics 134 (3) (2012) 031003. doi:10.1115/1.4005823.
URL http://vibrationacoustics.asmedigitalcollection.asme.org/article.aspx?articleid=1471683